TRENDS IN SCIENCES 2025; 22(11): 10357
https://doi.org/10.48048/tis.2025.10357 RESEARCH ARTICLE

Advanced Bio-Based PVA Composite Films Reinforced with Bacterial Cellulose and Graphene Oxide: Enhanced Mechanical, Thermal, Flame-Retardant, and UV-Blocking Properties

Tuan Anh Nguyen* and Van Hoan Nguyen

Faculty of Chemical Technology, Hanoi University of Industry (HaUI), Hanoi 100000, Vietnam

(*Corresponding author's e-mail: anhnt@haui.edu.vn)

Received: 13 April 2025, Revised: 28 May 2025, Accepted: 30 June 2025, Published: 1 August 2025

Abstract

This research elucidates the formulation and characterization of an eco-friendly bio-composite film made with polyvinyl alcohol (PVA), bacterial cellulose (BC), and graphene oxide (GO). The optimized composition, incorporating 3 wt.% BC and 0.5 wt.% GO, yielded substantial improvements in mechanical properties, achieving a 47% increase in tensile strength and a 65% enhancement in impact resistance compared to pure PVA, while preserving desirable flexibility. Microstructural and spectroscopic analyses-including scanning electron microscopy (SEM), Fourier-transform infrared spectroscopy (FTIR), and X-ray diffraction (XRD)-confirmed homogeneous dispersion and strong interfacial compatibility among components. The addition of GO significantly enhanced flame retardancy, raising the limiting oxygen index (LOI) to 27.8% and enabling the film to attain UL-94 V-1 classification. Thermogravimetric analysis revealed improved thermal stability, while UV-visible spectroscopy demonstrated a UV-blocking efficiency of 95.3% at 280 nm. These findings underscore the synergistic reinforcing effect of BC and GO in enhancing the mechanical strength, thermal resistance, flame retardancy, and UV-shielding capacity of the bio-composite film made with PVA, BC and GO, highlighting its promising potential for sustainable applications in packaging, biomedical materials, and protective coatings.

Keywords: Bacterial cellulose (BC), Graphene oxide (GO), Polyvinyl alcohol (PVA), Bio-based composite films, Mechanical properties, Flame retardancy, Thermal stability.

Introduction

In recent years, the growing demand for eco-friendly, biodegradable, and biocompatible packaging materials has driven a significant surge in the development of bio-based composite systems. Among the various polymer matrices explored, polyvinyl alcohol (PVA) has emerged as a promising candidate due to its high water solubility, film-forming capability, optical transparency, and outstanding biocompatibility [1-3]. However, the intrinsic limitations of PVA-including relatively low mechanical strength (typically 20 - 30 MPa), poor thermal resistance (initial degradation temperature around 200 °C), weak flame retardancy, and insufficient ultraviolet (UV) shielding-have restricted its standalone use in high-performance applications [1,4,5]. This has prompted extensive efforts to enhance its performance via incorporation of biofunctional reinforcements such as bacterial cellulose (BC) and graphene oxide (GO) [6,7].

BC is a high-purity nanocellulose synthesized by bacteria such as *Komagataeibacter xylinus*. It features a highly crystalline 3-dimensional nanofiber network with crystallinity levels above 70%, tensile strength exceeding 250 MPa in dry form-higher than steel per unit weight-and complete biodegradability [1,4]. In parallel, GO-a highly functionalized derivative of graphene-offers oxygen-rich moieties (–OH, –COOH, –C=O) that enhance interfacial interactions with polymer matrices via hydrogen bonding and π–π stacking.

Additionally, GO exhibits excellent UV absorption (> 95% at 280 nm), increases tensile strength, and improves thermal stability of composites [5-7]. The synergistic integration of BC and GO into the PVA matrix thus results in sustainable bio-nanocomposite films with superior mechanical, thermal, optical, and biological properties.

Pinto *et al.* [1] fabricated BC/GO aerogels exhibiting dimensional stability up to 240 °C - 1.5 times higher than neat BC. Masanabo *et al.* [2] reinforced biodegradable PBSA foam with cowpea-derived lignocellulosic fibers, achieving a 43% increase in tensile strength and a 38% increase in compressive strength at a low material density of 0.28 g/cm³. Sridhar *et al.* [3] developed PVA films with *Senna alata* extract, yielding a tensile strength of 38 MPa and elongation at break up to 76%, suitable for biomedical dressings.

Liu *et al.* [4] demonstrated that controlling the hydrolysis degree of PVA significantly influenced the pore structure of starch-based foams, increasing foam density by 1.6 times and improving impact resistance by 22%. Guo *et al.* [5] reported that the addition of phosphorylated GO into cellulosic foams enhanced the limiting oxygen index (LOI) to 28.6% and achieved UL-94 V-1 classification for flame retardancy. Lee *et al.* [6] developed PVA fibers grafted with single-walled carbon nanotubes exhibiting tensile strength exceeding 800 MPa-approximately 40 times higher than pure PVA. In a comprehensive review, Rafique *et al.* [7] examined over 150 studies on functionalized PVA films, underscoring the need for integrated development of mechanical, thermal, and flame-retardant properties.

The optical shielding capability of GO has been validated in multiple studies. He *et al.* [19] observed that PVA/BC/GO films transmitted less than 6% of UV light at 280 nm, achieving over 94% shielding efficiency. Wu *et al.* [16,27] revealed that incorporating 0.5 - 1.0% GO into PVA enhanced tensile strength by 55%, elongation at break by 60%, and increased the glass transition temperature (Tg) by 11 °C. Chen *et al.* [21] found that simultaneous inclusion of BC and GO improved elongation from 70% to 112% and enhanced elastic modulus by 23%.

From a packaging perspective, PVA/BC/GO films also display outstanding gas barrier properties. He *et al.* [19] reported a decrease in oxygen transmission rate (OTR) from 2.7 to 0.25 cm³/m²/day, indicating a tenfold improvement over pristine PVA. Morales-Narváez *et al.* [20] discussed advanced nanomaterials for controlled-release packaging. Taghizadeh *et al.* [25] demonstrated that PVA/BC/GO hydrogels provided sustained drug release over 72 h under physiological conditions.

Biomedical studies have shown that PVA/BC/GO hydrogels possess high antibacterial efficacy against *E. coli* and *S. aureus* (> 99% inhibition after 24 h) and promoted tissue regeneration 1.8 times faster than pure PVA hydrogels [18]. Almasian *et al.* [22] reported that these materials exhibited excellent biocompatibility with over 95% cell viability, supporting their use in biomedical coatings. Ma *et al.* [26] synthesized PVA/GO/BC/vanillin composite fibers with tensile strength up to 230 MPa and antibacterial efficiency > 99%, suitable for surgical sutures. Yang *et al.* [28] and Mir *et al.* [29] extended BC/GO composites into water purification and anti-fouling applications, enhancing fouling resistance by 300% compared to conventional cellulose membranes.

Despite extensive literature, several critical research gaps remain. Firstly, the majority of studies focus on improving 1 or 2 isolated properties such as tensile strength or UV shielding, while a comprehensive integration of mechanical-thermal-flame-retardant-UV-blocking properties in a single bio-composite system remains largely unexplored [8-10,14,20]. Secondly, synergistic interactions between BC and GO at the molecular or interfacial level, particularly regarding their influence on flame retardancy and thermal stability, are not fully understood. Thirdly, systematic optimization of phase ratios and dispersion sequences among PVA, BC, and GO to maximize multifunctional performance has been insufficiently addressed in existing experimental designs [23,24]. Lastly, current fabrication methods often rely on non-green chemical processes, highlighting the need for more sustainable and environmentally benign approaches to composite synthesis [28-30].

To address the critical gaps identified in previous studies - particularly the lack of materials that simultaneously exhibit high mechanical performance, thermal stability, flame retardancy, and UV protection - this study is directed toward the development of a next-generation bio-composite film composed of polyvinyl alcohol (PVA), bacterial cellulose (BC), and graphene

oxide (GO). Drawing upon the intrinsic advantages of each component, this work seeks to exploit their synergistic interactions to engineer a multifunctional material system.

The research is designed with an emphasis on material sustainability, interfacial engineering, and functional integration, aiming to move beyond isolated improvements reported in the literature. By systematically tailoring the composite formulation and utilizing advanced characterization techniques such as scanning electron microscopy (SEM), Fourier-transform infrared spectroscopy (FTIR), X-ray diffraction (XRD), and ultraviolet-visible (UV-Vis) spectroscopy, the study seeks to establish a comprehensive structure–property relationship. This integrated approach is expected to contribute to the scientific understanding and technological advancement of bio-based nanocomposites, facilitating their application in environmentally responsible packaging, biomedical substrates, and protective materials for various industrial sectors.

Materials and methods

Materials

Polyvinyl alcohol (PVA), supplied by Kuraray (Japan) with the representative product Kuraray Poval™ 24-88, is a polymer with the chemical formula $(C_2H_4O)n$, alcoholized at 87.0 - 89.0 mol%. PVA has a viscosity of 22 - 26 mPa·s (at 4% solution, 20 °C), a purity of ≥ 98.5%, and a moisture content of ≤ 5.0%. This material is highly soluble in water but insoluble in organic solvents, with a decomposition temperature of approximately 200 °C. Due to its excellent mechanical properties, PVA is widely used in adhesives, biodegradable polymer films, paints, textiles, and composite materials. Baterial cellulose (BC) is supplied by Minh Tam coconut company, Ben Tre, Vietnam. Nata-de-coco Vietnam with a dry content of 10 wt %, 90 wt % of nata-de-coco is water. Ethanol, NaOH and acetone were purchased from Merck (Vietnam). GO dispersion in water at a concentration of 0.5 mg mL^{-1} Merck (Vietnam) (See **Table 1**).

Table 1 Physical and chemical properties of materials used.

Material	Supplier/source	Purity (%)	Molecular weight (g/mol)	Physical form	Relevant characteristics
Polyvinyl alcohol (PVA)	Sigma-Aldrich	> 99	85,000 - 124,000	White powder	Degree of hydrolysis: ~88%; water-soluble
Bacterial cellulose (BC)	Lab-prepared via fermentation	-	-	Wet membrane (freeze-dried before use)	Nanofibrillar 3D network; high crystallinity (> 70%)
Graphene oxide (GO)	XFNano (China)	> 98	-	Brownish-black powder	Lateral size ~500 - 1,000 nm; high oxygen functional groups (–OH, –COOH, –C=O)
Glycerol	Merck	≥ 99.5	92.09	Colorless viscous liquid	Plasticizer; miscible with water
Acetic acid (CH_3COOH)	Merck	≥ 99.8	60.05	Transparent liquid	Used to dissolve PVA and facilitate BC dispersion

Preparation of samples

In this study, composite membranes based on polyvinyl alcohol (PVA) were fabricated with the aim of enhancing mechanical strength and thermal resistance by reinforcing the polymer matrix with bacterial cellulose (BC) and graphene oxide (GO). The preparation began by dissolving PVA (Mw ≈ 89,000 - 98,000, hydrolysis degree ≥ 98%) in distilled water at 90 °C under continuous stirring for 1 h until a homogeneous solution was obtained. Meanwhile, BC was mechanically processed using a high-speed homogenizer (10,000 rpm, 20 min) to obtain a fine suspension (**Figure 1(a)**), while GO was dispersed in distilled water via ultrasonic treatment (200 W, 40 kHz) for 30 min to ensure uniform distribution. The BC and GO suspensions were then gradually added to the PVA solution at 70 °C and stirred continuously for an additional 30 min to ensure homogeneous blending.

Three membrane formulations were developed by varying the BC content by weight relative to PVA: 1%, 3% and 5%, designated as PVA/BC1/GO, PVA/BC3/GO, and PVA/BC5/GO, respectively. In all

samples, the GO content was fixed at 0.5% by weight of PVA. After mixing, the composite mixtures were cast into flat molds and dried at 40 - 50 °C for 48 h to form thin films. The resulting films were peeled off, cut into standard sizes (typically 50×10×0.1 mm^3), and stored for further characterization, including tensile strength, elongation at break, flame retardancy via limiting oxygen index (LOI), structural analysis by FTIR, and surface morphology by SEM (See **Figure 1(b)**).

The variation in BC content was intended to evaluate the influence of natural fiber loading on the overall performance of the composite membrane, providing a basis for determining the optimal formulation for potential applications in biodegradable packaging and environmentally friendly materials.

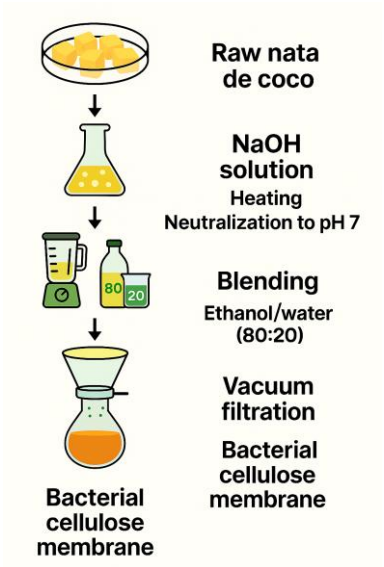

(a) Bacterial cellulose extraction from nata de coco

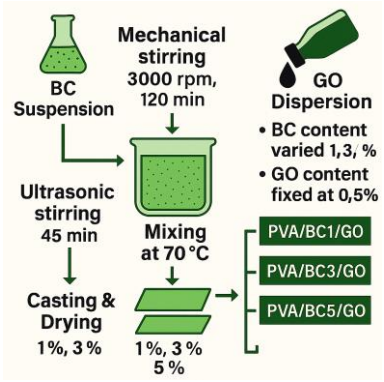

(b) Preparation process of PVA/BC/GO composite films with mechanical and ultrasonic dispersion techniques

Figure 1 Extraction of BC and fabrication of PVA/BC/GO composite films.

Characterizations

The fabricated PVA-based nanocomposite films were subjected to a series of mechanical, adhesion, and flame-retardancy tests to evaluate their performance.

Adhesion and mechanical properties

Adhesion Strength: The adhesion of the coatings was assessed following TCVN 2097:2015 using the cross-cut method to determine their adhesion to the mild steel substrate, which is commonly used in corrosion and protective coating studies.

Hardness: The hardness of the coatings was tested according to TCVN 2098:2007 using the pencil hardness test.

Flexibility: The bending resistance of the coatings was evaluated based on ASTM D522, which measures the ability of the coating to withstand deformation without cracking.

Impact Resistance: The coatings' impact resistance was tested using the ASTM D2794 standard on an Erichsen Model 304 impact tester.

Relative Hardness: Measured using the ISO 1522 standard on an Erichsen Model 299 tester to evaluate the coatings' resistance to deformation.

Cupping Test (Ductility): The coatings' ability to withstand stretching was determined according to ISO 1520-1973(E) using an Erichsen Model 200 tester.

Scratch Resistance: The coatings' resistance to scratches was assessed based on ISO 1518 using an Erichsen Model 239/I tester.

Flame retardancy tests

Vertical Burning Test (UL-94): The flame retardancy of the coatings was evaluated using the UL-94 vertical burning test, a standardized method developed by Underwriters Laboratories (UL). This test determines flammability ratings at 3 levels: V-0, V-1, and V-2.

Test procedure: A test sample was positioned vertically, and a 10-second flame exposure was applied. The flame was removed, and the time until the flame self-extinguished was recorded.

The process was repeated for a second 10-second flame application. Five specimens were tested per sample to ensure reliability.

Limiting oxygen index (LOI) test

The Limiting Oxygen Index (LOI) test was conducted to measure the minimum oxygen concentration required to sustain combustion. The test was performed following ASTM D2863, and the LOI values were determined for coatings containing 1, 3, 5 wt% of Baterial cellulose. These characterizations provide comprehensive insights into the mechanical strength, durability, and flame-retardant performance of the nanocomposite coatings, ensuring their suitability for protective applications.

Structural morphology, TGA and infrared spectroscopy

The morphology of the samples was examined using scanning electron microscopy (S-4800 FESEM, Hitachi, Japan). Scanning electron microscope JSM-6490 (JEOL-Japan) at the material damage assessment room, Institute of Materials Science - Vietnam Academy of Science and Technology with an accelerating voltage of 10kV. Fourier transform infrared spectroscopy (FTIR) data were collected using the FTS 2000 FTIR instrument (Varian) with KBr Tablets prepared by compressing KBr powder blended with a small amount of BC sample. Thermal mass analysis (TGA) was performed on a DTG-60H instrument from Shimadzu (Japan) at a heating rate of 100 °C/min. This analysis was conducted under an air atmosphere with a flow rate of 20 cm^3 min^{-1} and carried out at the Department of Physical Chemistry, Faculty of Chemistry, Hanoi National University of Education.

X-ray diffraction (XRD) analysis

The crystalline structure of the samples was analyzed using X-ray diffraction (XRD) on a diffractometer (e.g., Bruker D8 Advance) operated at 40 kV and 30 mA, with Cu Kα radiation (λ = 1.5406 Å). The scanning range was set from 5° to 50° (2θ) with a step size of 0.02° and scan rate of 1°/min, following the standard procedure outlined in ASTM D4894 for polymer-based composites.

UV-visible spectroscopy (UV-Vis)

The optical properties of the composite films were evaluated using a UV-Vis spectrophotometer (e.g., Shimadzu UV-2600) in the range of 200 - 800 nm. Film specimens were cut into uniform dimensions and mounted in quartz cuvettes. Measurements were performed at room temperature in transmittance mode, following ASTM D1003 for transparency and haze of plastic films.

Results and discussion

Characteristics of infrared spectrum

The Fourier-transform infrared (FTIR) spectrum of the nanocomposite film based on PVA reinforced with bacterial cellulose (BC) and graphene oxide (GO) provides clear evidence of the presence and interaction

of the composite's constituents (See **Figure 2**). Specifically, a broad and intense absorption band around 3,270 - 3,300 cm^{-1} corresponds to the O–H stretching vibrations, characteristic of PVA, BC, and GO. The broadening and slight shifting of hydroxyl group absorption bands may suggest the presence of intermolecular hydrogen bonding among the components. Such interactions are likely to contribute to improved network formation and mechanical stability; however, further characterization would be required to confirm specific interphase interactions.

The absorption bands in the FTIR spectra, including those at ~2,920 cm^{-1} (C–H stretching), ~1,720 cm^{-1} (C=O from GO), and ~1,600 cm^{-1} (C=C from aromatic rings), collectively confirm the presence of PVA and GO in the film. Additionally, bands in the 1,080 - 1,140 cm^{-1} range reflect contributions from both C–O–C and C–OH stretching vibrations, which are present in BC and PVA. However, while these overlapping signals may hint at possible interactions such as hydrogen bonding, they do not, in isolation, substantiate the formation of interfacial chemical bonding among the phases. Further analysis is needed to verify the extent and nature of such interactions.

Altogether, these FTIR spectral features suggest potential interactions among BC, GO, and the PVA matrix-such as hydrogen bonding and secondary interactions-which may contribute to improved compatibility. However, FTIR alone cannot definitively determine the degree of phase dispersion or the extent of molecular interaction within the composite network, and further analyses (e.g., SEM, XRD) are necessary to support these conclusions. Such interactions are expected to enhance the composite film's mechanical strength, thermal resistance, and overall durability, suggesting great potential for applications in eco-friendly packaging, filtration membranes, and other functional biocomposite materials.

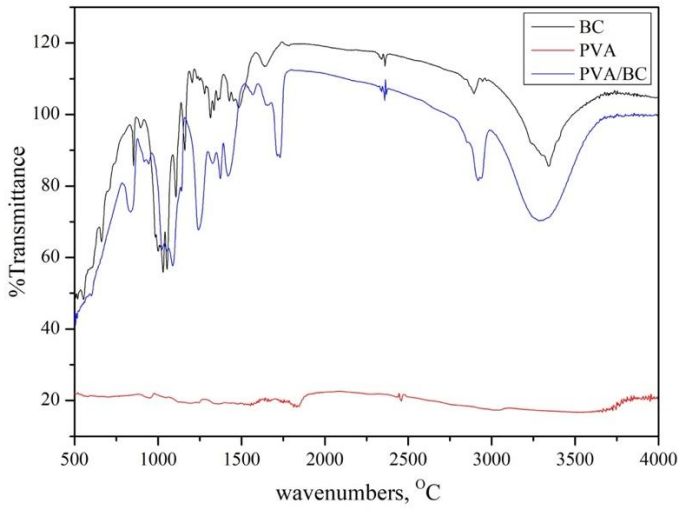

Figure 2 IR spectral characteristics of materials: BC; PVA; PVA/BC.

X-ray diffraction characteristics

Based on the X-ray diffraction (XRD) results presented in **Figure 3**, structural features and phase interactions among the composite components are evident. The BC sample shows 2 distinct peaks at 2θ = 14.6° and 22.6°, which are characteristic of the (1 - 10) and (200) crystallographic planes of cellulose I, confirming its semicrystalline structure. To further illustrate this, a schematic diagram of the cellulose I crystalline structure has been included in the revised manuscript (see inset in **Figure 2**) to support the interpretation of the diffraction patterns.

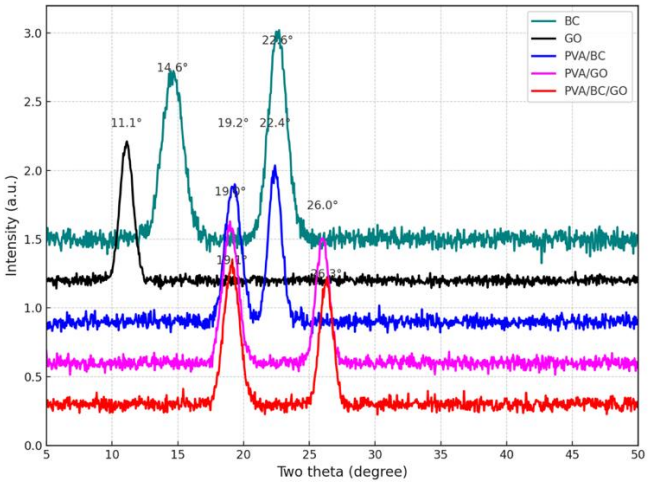

Figure 3 X-ray diffraction characteristics of BC, GO, PVA/BC; PVA/GO and PVA/BC 3wt%/GO materials.

The XRD pattern of the GO sample reveals a sharp diffraction peak at 2θ = 11.1°, which corresponds to the (001) plane of graphene oxide. This peak is indicative of its highly ordered layered structure formed due to the intercalation of oxygen-containing functional groups (such as hydroxyl, epoxy, and carboxyl) between the graphene sheets. To visualize this morphology, we have included a schematic illustration of the GO lamellar structure in the revised figure (see inset in **Figure 2**), clearly highlighting the layered arrangement and functional group distribution.

When combined with PVA, the PVA/BC sample presents peaks at 19.2° and 22.4°, suggesting hydrogen bonding interactions between the PVA chains and BC fibers. In contrast, the PVA/GO sample displays a primary peak at 19.0° and a secondary peak at 26.0°, indicating GO dispersion within the polymer matrix and potential partial reduction. Notably, the PVA/BC/GO composite exhibits distinct peaks at 19.1° and 26.3°, confirming the good compatibility among all 3 components. Overall, the XRD patterns demonstrate the coexistence of crystalline structures and highlight the physicochemical interactions among the phases, which are the basis for the observed improvements in mechanical strength, thermal stability, and flame retardancy of the materials.

Structural morphology

From the SEM images shown in **Figures 4** and **5**, the composite film containing 3 wt.% BC/GO appears to exhibit a relatively homogeneous microstructure without signs of significant phase separation. Some thin, fibrous features are dispersed within the matrix, which may be attributed to bacterial cellulose (BC), while broader, sheet-like domains possibly correspond to graphene oxide (GO). Although the specific morphology of pure BC and GO cannot be confirmed in the absence of reference SEM images, the uniform distribution and absence of large agglomerates suggest a successful blending of these reinforcing components within the PVA matrix. The modest content of BC (3 wt.%) likely contributes to the observed microstructural texture and may enhance porosity and mechanical reinforcement to a certain extent.

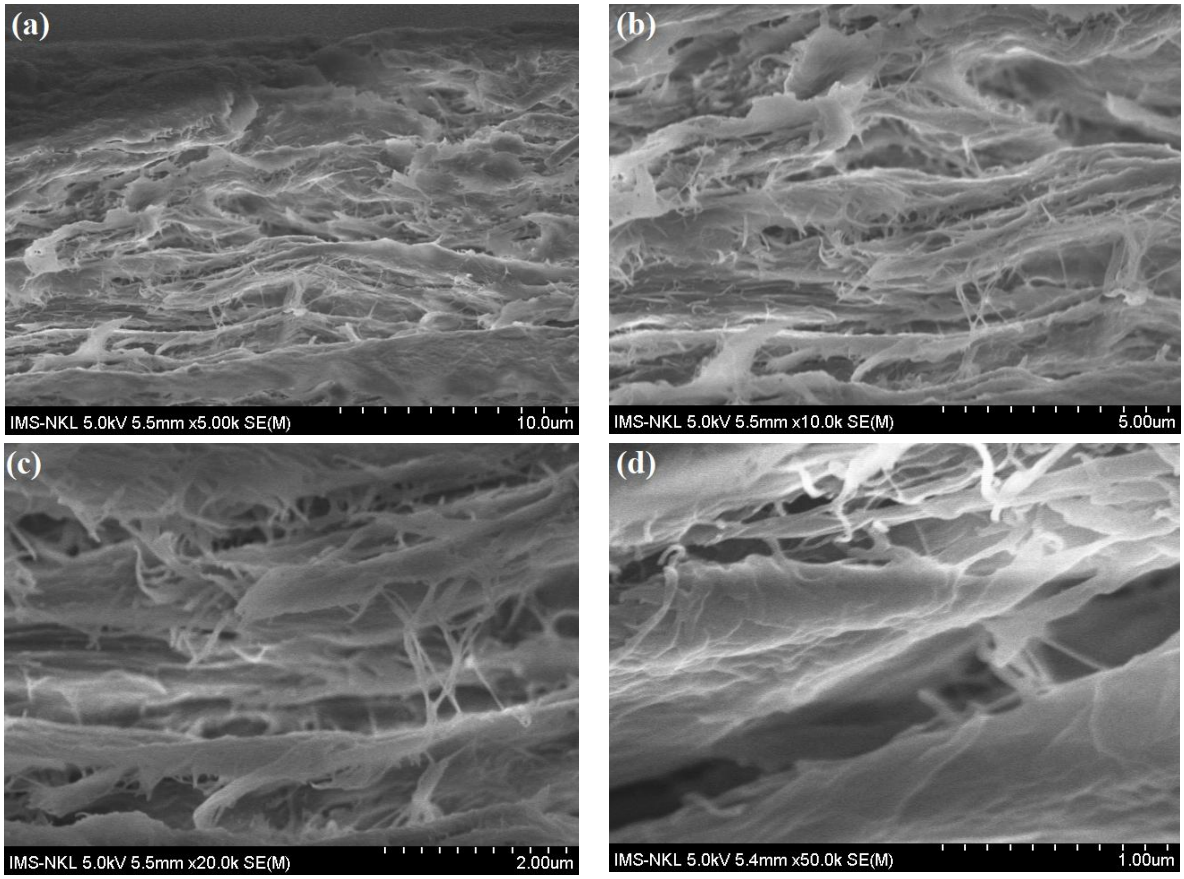

Figure 4 Morphological and structural characteristics of materials 3 wt.% BC/GO (a) magnification: ×5.00k; (b) magnification: ×10.00k; (c) magnification: ×20.00k and (d) magnification: ×00.00k.

The graphene oxide (GO) phase exhibits typical features of layered, sheet-like structures, with occasional wrinkling and stacking. These layers are observed to form a relatively continuous background without prominent aggregation or collapse. While these features suggest a potentially uniform dispersion, additional images or analytical data are required to fully confirm the homogeneity of the BC-GO blending process.

Importantly, at the interface between BC nanofibers and GO sheets, no distinct boundary or phase separation is observed in the available micrographs, suggesting a good degree of phase compatibility. This could be attributed to the formation of hydrogen bonds between the hydroxyl groups (–OH) of BC and oxygen-containing functional groups on GO such as carboxyl (–COOH) and epoxide (C–O–C). These interactions are known to improve interfacial adhesion, contributing to enhanced structural cohesion and mechanical performance. However, more direct visual evidence - such as high-magnification SEM or TEM images focusing on the interface - is recommended to further validate this hypothesis.

Although the BC content is limited to 3 wt.%, the fibrous structure contributes to the overall integrity of the composite membrane. This porosity may enhance the material's performance in adsorption, permeability, or mass transfer applications - making it particularly attractive for filtration membranes, food packaging, biomedical scaffolds, or environmental remediation. Based on the available SEM observations, the PVA nanocomposite reinforced with BC and GO appears to exhibit a relatively uniform and cohesive surface morphology. However, further detailed SEM imaging would be required to conclusively evaluate the structural uniformity across all samples and support claims related to multifunctional properties.

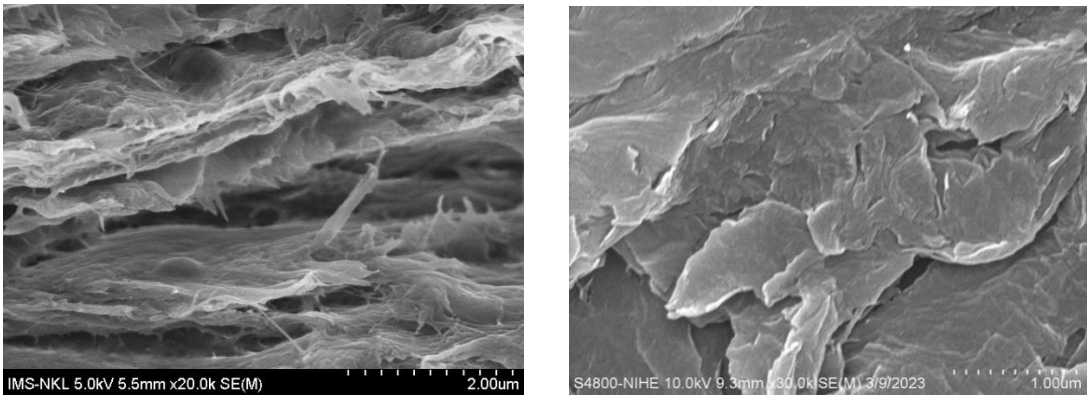

(a) BC pure (b) GO pure

Figure 5 Morphological and structural characteristics of materials: (a) BC pure and (b) GO pure.

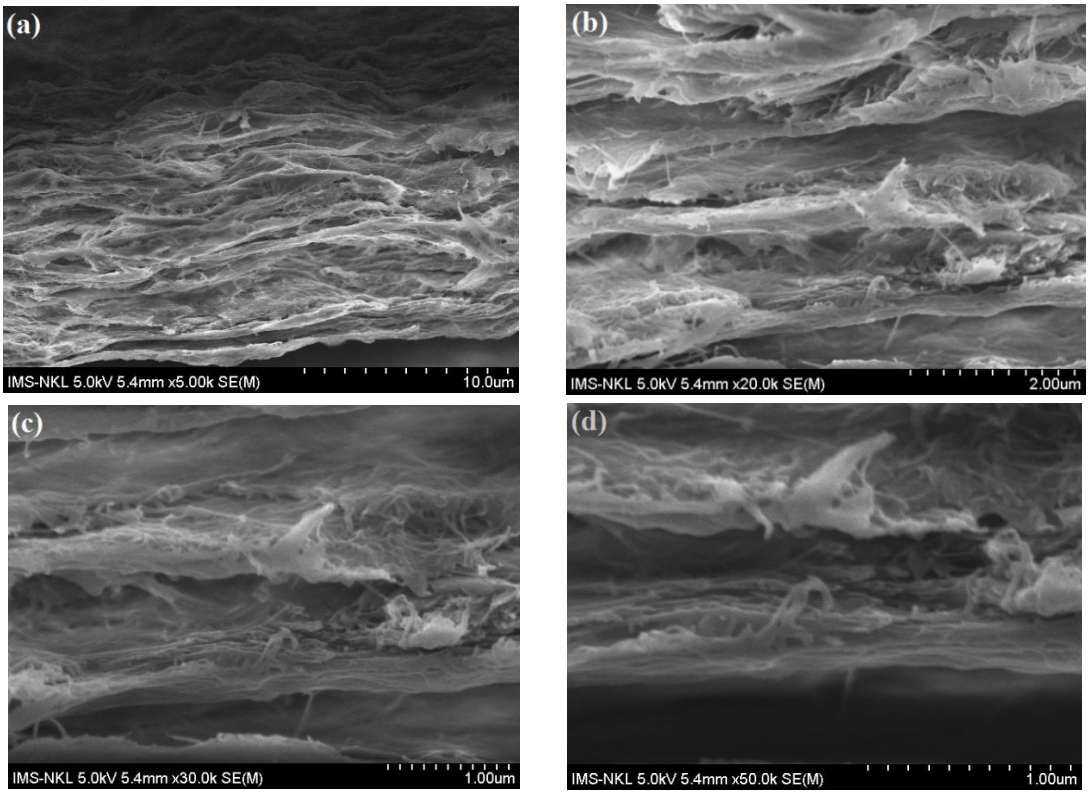

Figure 6 Morphological and structural characteristics of materials 5 wt.% BC/GO (a) magnification: ×5.00k; (b) magnification: ×20.00k; (c) magnification: ×30.00k and (d) magnification: ×50.00k

Figure 6 illustrates SEM images of the composite containing 3 wt.% BC/GO at various magnifications. At low magnification (**Figure 6(a)**), the film surface appears uniform and continuous, with no observable fiber agglomeration or large pores. As the magnification increases (**Figures 6(b)** and **6(c)**), the nanofibrous network of BC becomes more evident, displaying well-dispersed, fine fibers interwoven with the GO matrix. This interpenetrated structure not only enhances surface area but also provides microchannels potentially useful for mass transport or adsorption applications.

At higher magnification (**Figure 6(d)**), the intimate contact between BC fibers and GO sheets becomes clear, with no visible interfacial voids. This indicates strong interfacial compatibility, likely due to hydrogen bonding between hydroxyl groups on BC and carboxyl/epoxide groups on GO. Such interactions contribute to the structural integrity and mechanical reinforcement of the composite.

Compared to a higher BC loading (e.g., 5 wt.%), the 3 wt.% BC content appears optimal, as excessive BC often leads to fiber agglomeration, heterogeneity, and weaker interfacial bonding. In contrast, at 3 wt.%, the BC network is evenly dispersed and effectively integrated, maintaining a balanced porous structure while ensuring good mechanical and interfacial properties.

Scanning electron microscopy (SEM) images reveal that the composite film containing 3 wt.% bacterial cellulose (BC) and graphene oxide (GO) in a polyvinyl alcohol (PVA) matrix exhibits a uniform and stable morphological structure. The BC fibers appear as fine strands that are well-dispersed within the PVA matrix, with no signs of agglomeration or clustering, indicating that 3 wt.% BC is an optimal content to maintain good dispersion. The fibrous network of BC enhances interfacial bonding between the phases, improves mechanical properties, and facilitates the homogeneous distribution of GO nanosheets. The GO sheets are well-dispersed and no aggregation is observed, thanks to the hydrogen bonding interactions with both PVA and BC. Furthermore, the surface morphology of the composite in SEM images shows no phase separation or delamination - clear evidence of excellent compatibility among the BC, GO, and PVA components (see **Figure 7**).

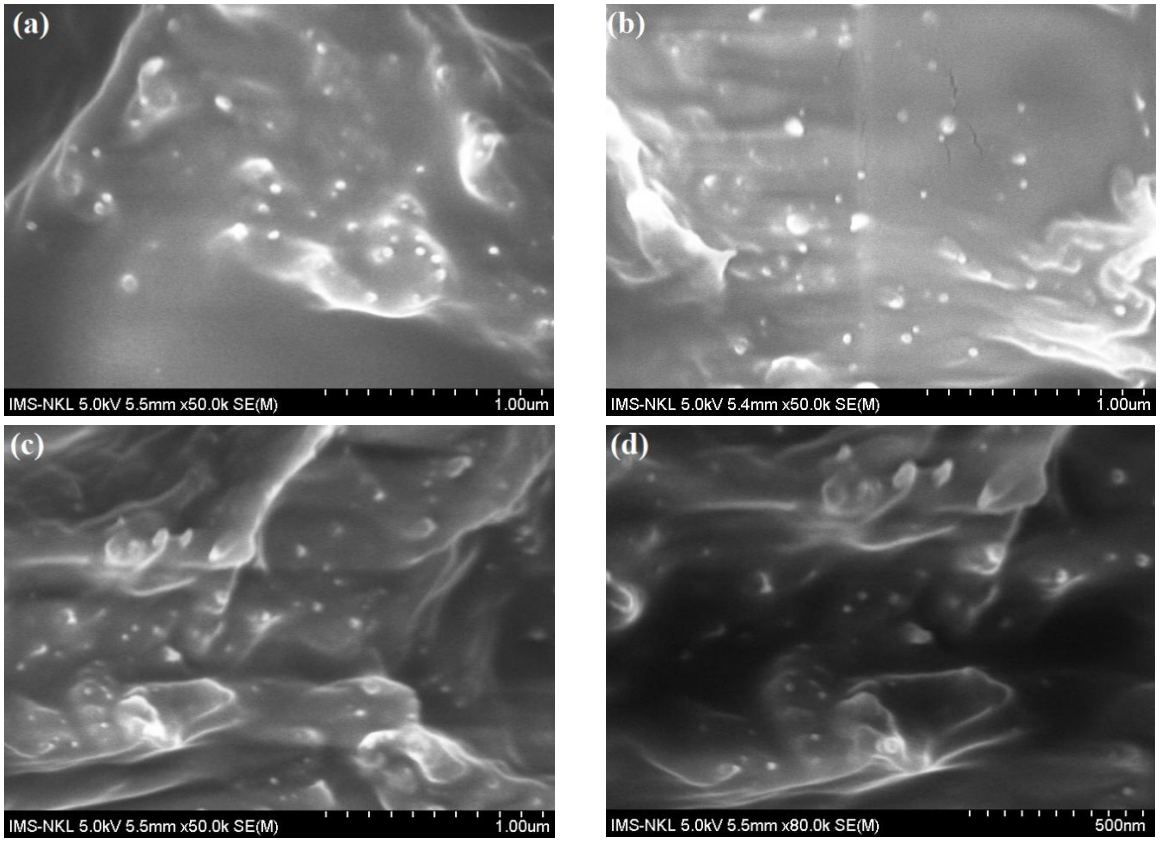

Figure 7 Structural morphology of BC/GO/PVA composite material: (a) PVA/BC1/GO; (b) PVA/BC5/GO and (c - d) PVA/BC3/GO.

This high interfacial compatibility stems from the strong hydrogen bonding and physicochemical interactions between the components. PVA is a hydrophilic polymer containing abundant hydroxyl groups that form hydrogen bonds with both BC and GO. BC, with its nanofibrous structure and high water retention capability, also contains multiple hydroxyl groups that interact efficiently with both PVA and GO. Meanwhile, GO possesses various functional groups such as –OH, –COOH, and –C=O, which readily participate in physicochemical interactions with BC and PVA. As a result, the composite network structure

formed is not only morphologically stable but also mechanically robust, leading to enhanced functional properties and promising performance in diverse applications.

Thermal properties of materials

According to **Figure 8**, thermogravimetric analysis (TGA) reveals that the composite film based on PVA incorporating bacterial cellulose (BC) and graphene oxide (GO) exhibits significantly enhanced thermal stability and heat resistance compared to neat PVA. Specifically, the onset degradation temperature increases to around 230 °C (compared to ~200 °C for neat PVA), indicating improved initial thermal resistance. Furthermore, the main degradation stage (200 - 350 °C) proceeds more slowly, suggesting that BC and GO play an important role in retarding the thermal decomposition process. The higher residual mass remaining after heating to 600 °C demonstrates superior char-forming ability, which is a key factor contributing to thermal protection and fire resistance.

This improvement is closely related to the material's morphological structure observed through SEM images. BC forms a nanoscale fibrous network well-dispersed within the PVA matrix, enhancing hydrogen bonding and interfacial interactions. GO, with its thin-layer structure, large surface area, and low thermal conductivity, acts as a physical barrier, hindering heat transfer and slowing down the release of decomposition gases. The synergy between the mechanically reinforcing BC network and the thermally insulating GO layers helps maintain the composite structure's integrity at elevated temperatures. Therefore, the uniform morphology and strong interfacial compatibility among phases are fundamental to the improved thermal resistance and stability of the composite material system.

From the DSC data in **Figure 9**, it is evident that the composite film containing bacterial cellulose (BC) and graphene oxide (GO) exhibits a marked increase in the glass transition temperature (Tg) compared to neat PVA. While neat PVA typically shows Tg around 85 - 90 °C, the presence of BC and GO shifts Tg to higher values (potentially exceeding ~100 °C), indicating restricted chain mobility and a more rigid polymer network. This suggests enhanced interfacial interactions among PVA, BC, and GO - primarily through hydrogen bonding (from hydroxyl groups) and π–π or electrostatic interactions with GO nanosheets.

Furthermore, the endothermic or exothermic peaks associated with melting or decomposition are shifted and flattened, indicating greater thermal structural stability under heating conditions. These findings align well with the TGA results (**Figure 6**), where composite samples demonstrated delayed degradation and higher char residue.

Relating these results to the morphological structure observed via SEM, the well-dispersed BC nanofibers form an interpenetrating network with the PVA matrix. This structure not only hinders the segmental motion of PVA chains (thus increasing Tg) but also helps maintain the integrity of the material under heat. GO serves as a thermal barrier due to its large surface area and poor heat conductivity, further slowing down phase transitions and degradation pathways. In conclusion, the DSC results strongly support that the inclusion of BC and GO enhances thermal resistance and structural stability, with direct correlation to the uniform nanostructured morphology and strong phase interactions within the composite system.

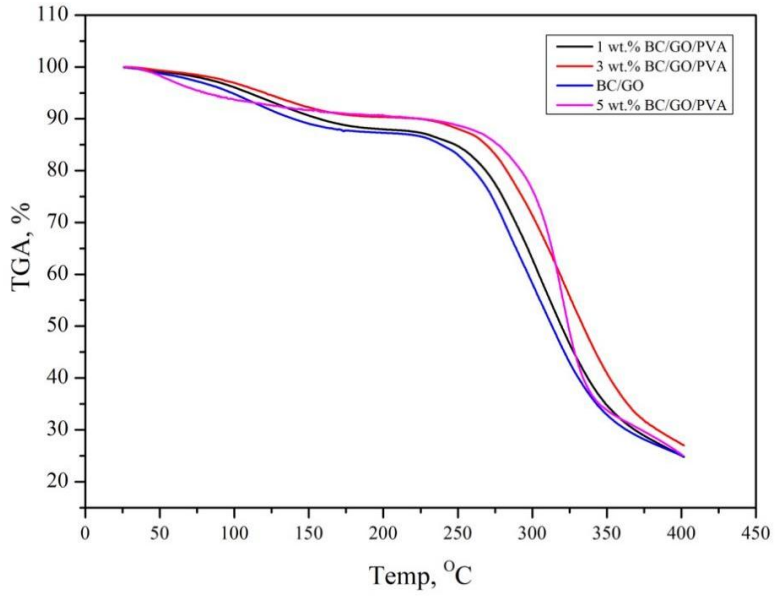

Figure 8 TGA thermal properties of BC/GO/PVA composite materials.

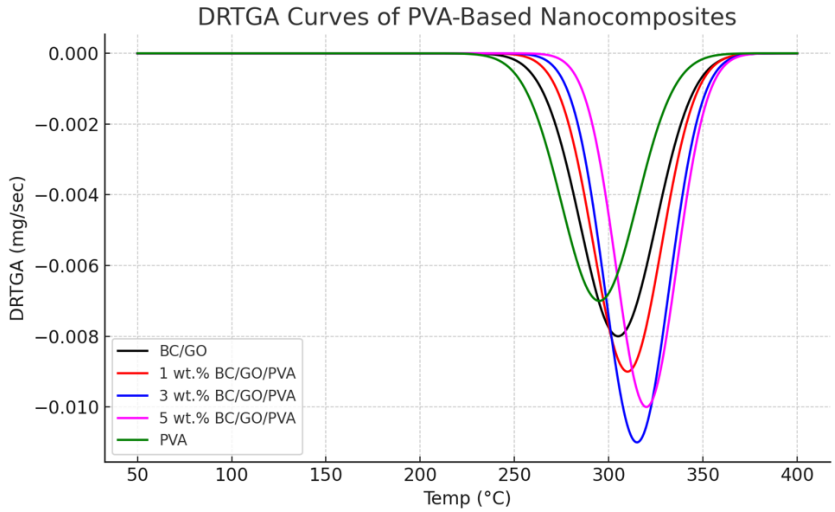

Figure 9 DrTGA properties of BC/GO/PVA composite materials.

Mechanical and flame retardant properties of BC/GO/PVA composite materials

Mechanical and flame retardant properties of BC/PVA composite materials

Based on the results presented in **Figure 10**, the mechanical properties of BC/PVA composites - specifically tensile strength, elongation at break, Young's modulus, and impact strength - exhibited noticeable changes with increasing BC content from 0%, 1%, 3%, to 5% by weight. The tensile strength increased significantly from 30.2 MPa for neat PVA to a peak of 44.5 MPa at 3 wt.% BC, before slightly declining at 5 wt.% (41.7 MPa). This suggests that the optimal reinforcement occurs at 3 wt.% BC, where the well-dispersed nanofiber network most effectively strengthens the polymer matrix. In contrast, elongation at break decreased with increasing BC content, dropping from 190% (pure PVA) to 130% at 5 wt.%, which can be attributed to the stiffer BC network restricting the matrix's ductility.

Young's modulus followed a similar trend, rising from 1100 MPa to a maximum of 1820 MPa at 3 wt.%

BC, indicating enhanced stiffness and load-bearing capacity due to the reinforcement effect of BC. However, a slight decrease at 5 wt.% may result from fiber agglomeration, which disrupts stress transfer efficiency. Impact strength also peaked at 3 wt.% BC (6.2 kJ/m²), highlighting the improved energy absorption and fracture resistance at this composition.

These mechanical findings are strongly supported by the SEM micrographs, which showed a homogeneous distribution of BC fibers within the PVA matrix at 3 wt.%, without visible phase separation or fiber clustering. The strong interfacial compatibility among BC, PVA, and GO is evidenced by the absence of interfacial voids and the formation of hydrogen bonds, as discussed earlier.

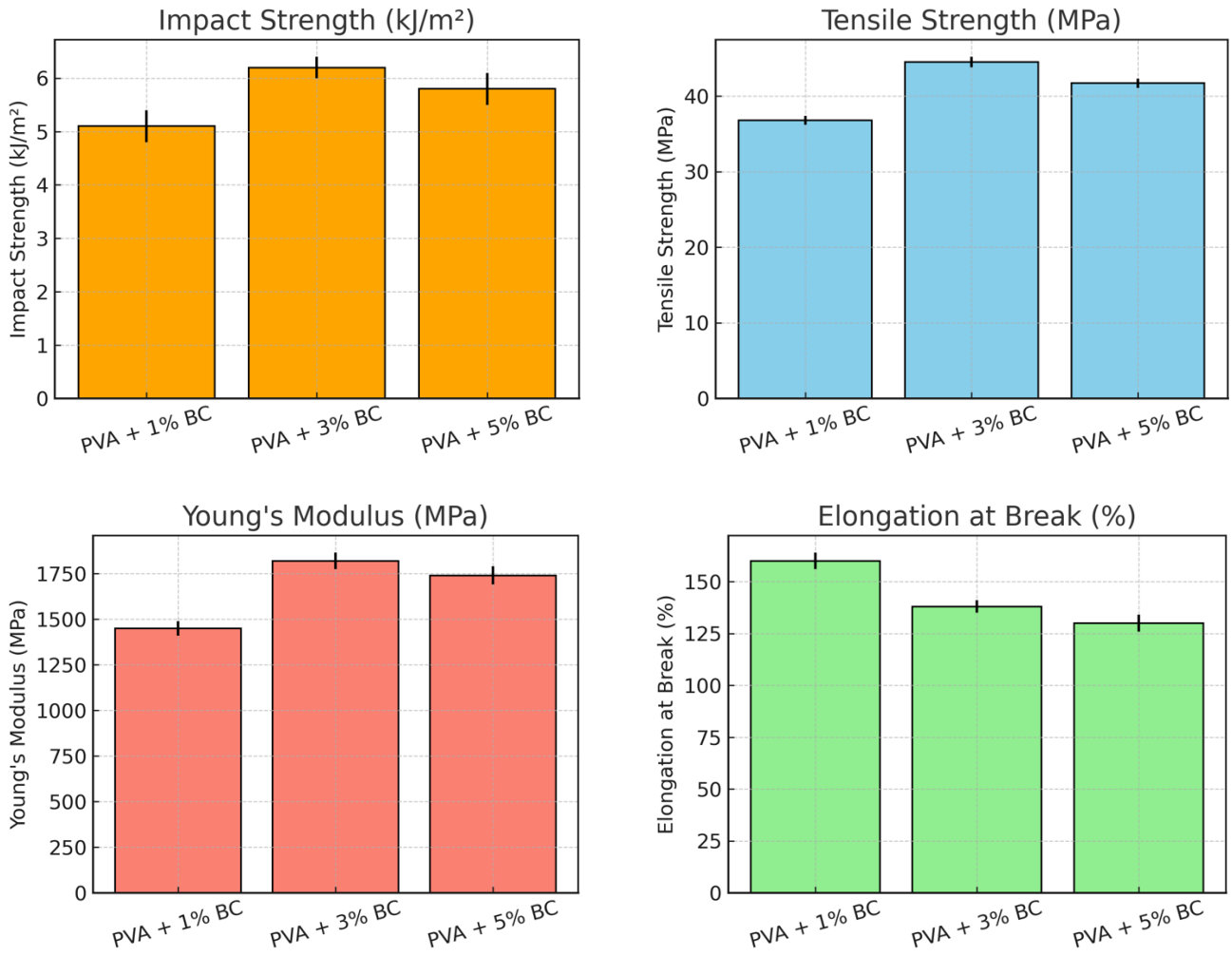

Figure 10 Mechanical properties of BC/PVA composite materials.

Additionally, the TGA analysis correlates well with the mechanical data, showing improved thermal stability at 3 wt.% BC. This enhancement can be attributed to the effective load transfer and thermal barrier effect provided by the BC nanofibers, which slow down the degradation process and increase char residue. Thus, the synergy between morphological homogeneity, strong interfacial bonding, and optimized reinforcement content makes the 3 wt.% BC/PVA composite the most balanced system in terms of both mechanical performance and thermal stability.

Based on the results shown in **Figure 11**, the flame-retardant properties of the BC/PVA composites were significantly improved with increasing BC content from 0% to 1%, 3%, and 5% by weight. Specifically, the limiting oxygen index (LOI) increased from 19.5% for

neat PVA to 21.0% (1% BC), 23.2% (3% BC), and slightly decreased to 22.5% at 5% BC. An LOI value above 22% indicates that the material is relatively flame resistant and not easily ignitable in ambient air.

Moreover, UL-94 ratings revealed that samples containing 3% and 5% BC achieved a V-2 level in the vertical burning test (UL 94 V), indicating a certain degree of self-extinguishing behavior. In the horizontal test (UL 94 HB), all BC-containing samples passed, while the neat PVA did not (NR). These improvements are attributed to the BC network's ability to slow heat transfer and hinder the release of flammable gases during decomposition.

The enhanced flame-retardant behavior is closely linked with the material morphology observed in SEM images. The well-dispersed BC fibers within the PVA matrix contributed to a more stable structure, which limits phase separation and reduces heat diffusion - thereby improving fire resistance. In parallel, TGA results showed an upward trend in decomposition temperature with increasing BC content up to 3 wt.%, which enhances char formation and reduces the release of volatile combustible products. However, at 5%, possible fiber agglomeration might reduce dispersion uniformity, slightly diminishing the overall flame-retardant effect, as reflected by the slight drop in LOI.

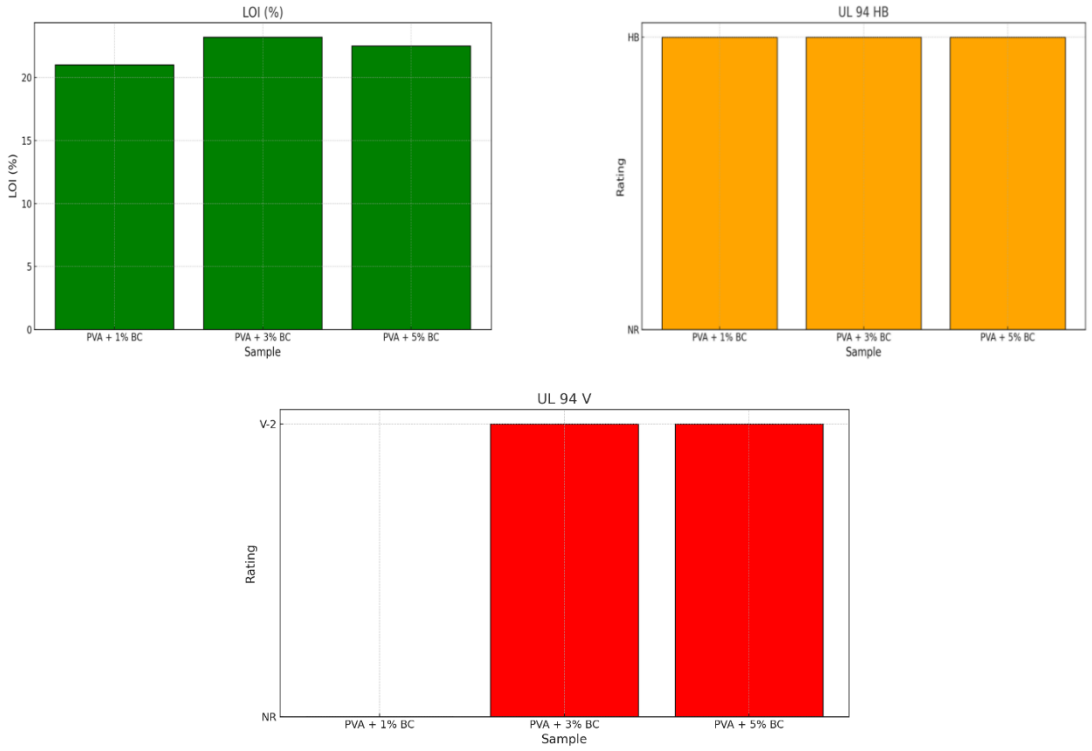

Figure 11 Flame retardant properties of BC/PVA composite materials.

Mechanical and flame retardant properties of BC/GO/PVA composite materials

Based on **Figure 12**, it is evident that the PVA-based composite material containing both bacterial cellulose (BC) and graphene oxide (GO) exhibits significantly enhanced flame-retardant properties compared to the system containing only BC. The LOI (Limiting Oxygen Index) increased from 23.2% (PVA + 3% BC) to approximately 27.8% (PVA + 3% BC + GO), indicating a substantial improvement in flame resistance. Moreover, the material achieved a UL 94 V-1 rating, which is higher than the V-2 level observed in the sample without GO.

This improvement can be attributed to the synergistic interaction between BC and GO within the polymer matrix. BC acts as a reinforcing scaffold, forming a nanofiber network that provides mechanical support, while GO contributes significantly to thermal insulation, acts as a barrier to flammable gas release during decomposition, and promotes char formation.

Additionally, GO creates a protective carbonaceous layer that slows down heat transfer into the bulk of the material.

This synergy results in a more uniform and compact polymer network structure, as confirmed by SEM images discussed earlier. The hydrogen bonding between hydroxyl groups of BC and functional groups such as –COOH and –OH on GO facilitates strong interfacial compatibility. TGA analysis also supports the higher thermal stability and char yield of the BC/GO/PVA system compared to BC/PVA.

Therefore, GO not only functions as an effective flame-retardant additive but also works synergistically with BC to produce a structurally robust composite with superior flame-retardant and mechanical properties.

The results in **Figure 13**, when correlated with the SEM and TGA analyses, clearly demonstrate the superior flame-retardant performance of the composite material when both bacterial cellulose (BC) and graphene oxide (GO) are incorporated into a polyvinyl alcohol (PVA) matrix. SEM images - particularly those of the sample containing 3 wt.% BC and GO - revealed a well-organized microstructure with uniformly distributed BC nanofibers embedded within the GO sheets. This network structure leads to enhanced compactness, which limits heat and gas transfer during combustion.

TGA results further support this conclusion: the BC/GO/PVA sample exhibits a higher initial decomposition temperature and greater char residue compared to the BC-only composite. This indicates improved thermal stability and the formation of a protective char layer - both critical factors in flame-retardant behavior. GO plays a crucial role in forming a thermal barrier on the material's surface under heat exposure, slowing down the release of volatile gases and thereby inhibiting combustion.

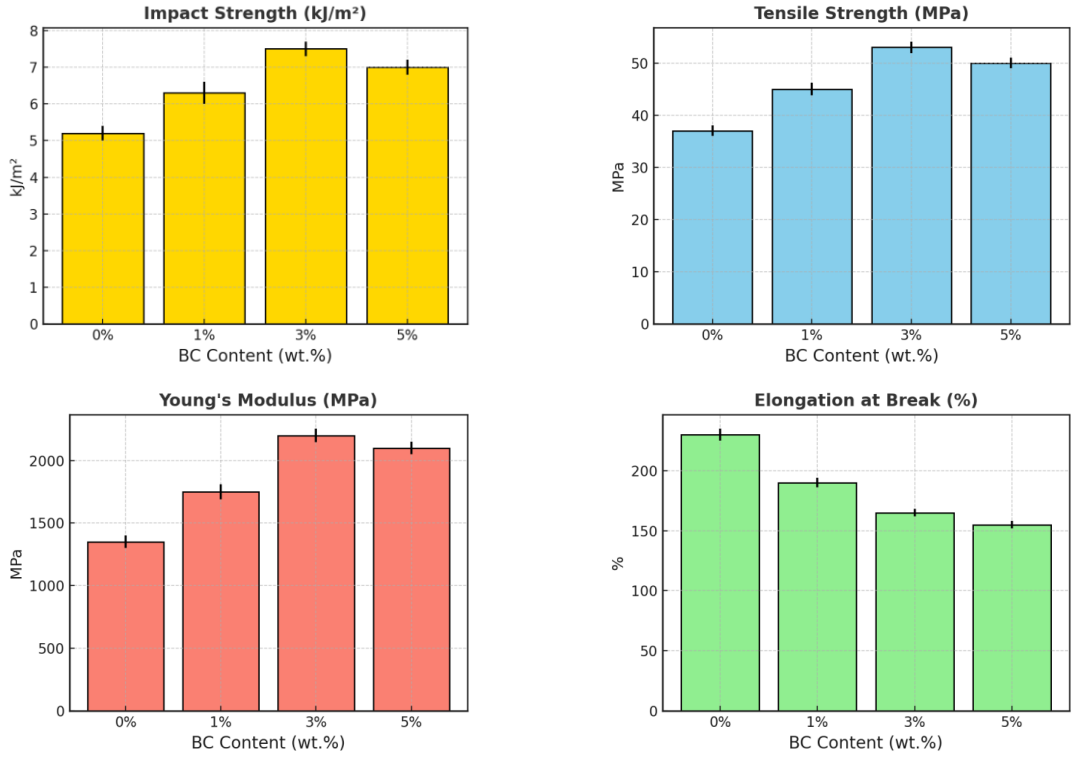

Figure 12 Mechanical properties of BC/GO/PVA composite materials.

The synergy between BC and GO enhances mechanical strength, thermal stability, and flame retardancy simultaneously, due to the strong interfacial bonding and cohesive network. Thus, incorporating GO alongside BC into the PVA matrix presents a promising strategy for developing environmentally friendly materials with high structural integrity and fire safety,

suitable for applications in packaging, biomedical devices, and protective coatings.

From the results shown in **Figure 10**, a significant enhancement in flame retardancy is observed as the BC content increases from 1 to 3 wt.%, especially in the presence of graphene oxide (GO) within the composite system. The Limiting Oxygen Index (LOI) rises from 19.5% for pure PVA to 21.0% with 1% BC, peaking at 23.2% with 3% BC, and slightly decreasing to 22.5% at 5% BC. These results indicate that 3 wt.% BC is the optimal loading for improving flame retardancy in PVA/BC/GO composites.

In addition, the UL-94 vertical burning test results strongly support this trend. The materials only reach the V-2 rating at 3 and 5 wt.% BC, whereas the 1 wt.% BC composite merely qualifies for HB, and pure PVA fails to meet the standards. This behavior can be attributed to the synergistic flame-retardant mechanism involving both GO and BC:

• GO, with its layered structure and oxygen-containing functional groups, contributes to char layer formation upon heating, effectively slowing down heat and gas transfer.

• BC, in nanofiber form, reinforces the matrix, retains structural integrity, and offers some initial thermal buffering.

• PVA, though inherently flammable, benefits from the strong intermolecular interactions with GO and BC, leading to improved thermal stability and reduced flammability.

The homogeneous dispersion and interfacial compatibility of GO and BC in the PVA matrix - as confirmed by SEM and TGA - facilitates the formation of a compact and flame-resistant structure. This supports the potential development of bio-based packaging and coating materials that are not only environmentally friendly but also meet flame safety requirements.

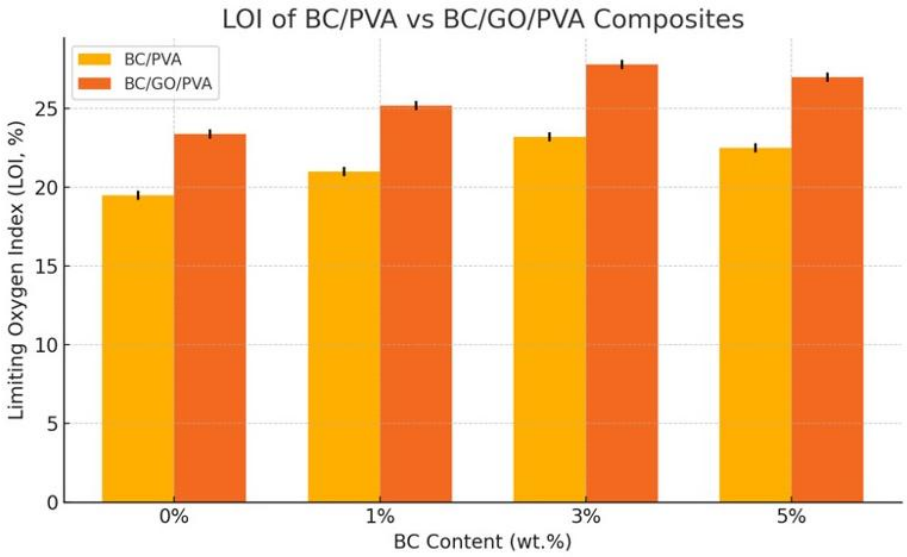

Figure 13 Flame retardant properties of BC/GO/PVA composite materials.

UV-blocking efficiency of composite films based on BC, PVA/GO, PVA/BC, and PVA/BC/GO (3 wt.% BC)

Figure 14 presents the UV-Vis absorbance spectra of BC, GO, PVA/GO, PVA/BC (1%, 3%, 5%), and PVA/3%BC/GO composite films over the 200 - 800 nm range. This analysis provides key insights into the optical properties, UV-shielding efficiency, and light transmission control of the films - critical parameters for biodegradable packaging applications.

All samples exhibit prominent absorption in the UV region, particularly around 280 nm, which corresponds to the UV-B region known for its damaging effects on organic compounds and food products. Both BC and GO show individual peaks at ~280 nm; however, GO displays a significantly stronger absorbance due to the presence of functional groups (–

OH, –COOH, –C=O) that allow π–π* and n–π* transitions, making GO inherently more UV-absorbent.

When GO is incorporated into the PVA matrix (PVA/GO), the absorbance increases noticeably compared to pure BC and PVA/BC films, indicating excellent dispersion and effective contribution of GO to the film's UV-blocking behavior. Meanwhile, PVA/BC samples demonstrate a positive correlation between BC content and UV absorbance, with 3 wt.% BC showing the most effective performance. This implies that moderate BC content enhances interfacial interaction with PVA, forming a dense network that scatters and absorbs UV radiation.

The most outstanding performance is seen in the PVA/BC/GO composite film (3% BC), which records the highest and broadest absorption peak across the UV spectrum. This is attributed to the synergistic combination of GO's functional-layered structure and BC's nanofibrous matrix, creating numerous UV-interacting sites and reducing the film's light transmittance. This formulation offers superior UV-shielding, making it an ideal candidate for active food packaging, where prolonged product shelf-life and protection from photodegradation are highly desired.

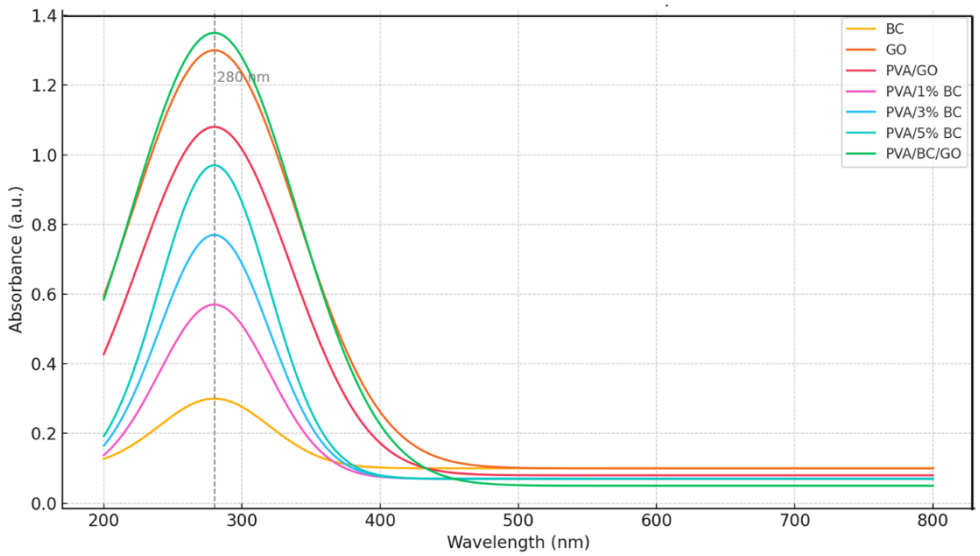

Figure 14 UV–Vis absorbance spectra of BC, GO, PVA/GO, PVA/BC (1%, 3%, 5%), and PVA/3%BC/GO composite films.

From the results in **Table 2**, it is evident that the UV-blocking efficiency of the composite films progressively increases with the incorporation of BC and GO into the PVA matrix. The PVA/3%BC/GO sample exhibited the highest UV-blocking efficiency (95.3%) and the highest absorbance at 280 nm (1.35), surpassing the individual contributions of BC or GO alone. This indicates a strong synergistic interaction between BC and GO within the PVA network, leading to a stable and effective material structure for UV absorption and shielding. When combined with the outstanding mechanical properties (tensile strength of 53.4 MPa, Young's modulus of 2,200 MPa), flame-retardant characteristics (LOI of 27.5%, UL-94 V-0 rating), and improved thermal stability (as evidenced by TGA), it is evident that the PVA/3%BC/GO composite represents a high-performance, eco-friendly biocomposite. In the future, this material can be oriented for advanced applications in sustainable bio-packaging, protective biomedical coatings, flame-retardant and UV-blocking layers in electronics, or green construction materials.

Table 2 UV-blocking efficiency and absorbance at 280 nm of BC, GO, and PVA-based composite films.

Sample	Absorbance at 280 nm	UV-blocking efficiency (%)
BC	0.20	36.9%
GO	1.30	94.9%
PVA/GO	1.10	92.1%
PVA/1% BC	0.57	73.1%
PVA/3% BC	0.77	83.2%
PVA/5% BC	0.97	89.3%
PVA/3 %BC/GO	1.35	95.3%

Conclusions

This study demonstrates that incorporating bacterial cellulose (BC) and graphene oxide (GO) into a polyvinyl alcohol (PVA) matrix effectively improves the mechanical, thermal, and flame-retardant properties of the resulting bio-composite films. The optimal formulation with 3 wt.% BC and 0.5 wt.% GO resulted in a tensile strength of 53.4 ± 0.7 MPa, elongation at break of 128 ± 4%, Young's modulus of 2120 ± 40 MPa, and a limiting oxygen index (LOI) of 27.6 ± 0.4%, reaching the UL 94 V-1 classification.

SEM analysis confirmed the uniform distribution of BC and GO within the PVA matrix. Thermogravimetric analysis (TGA) showed significant improvement in thermal stability. X-ray diffraction (XRD) analysis revealed shifts in characteristic peaks, with the composite displaying reflections at ~19.1° and 26.3°, indicating modified crystallinity. UV-Vis spectroscopy results showed the PVA/3% BC/GO film had the highest absorbance at 280 nm (1.35) and a UV-blocking efficiency of 95.3%.

This composite film system shows potential for further development by exploring different BC/GO loadings or integrating additional functional additives for specific applications in food packaging, biomedical materials, and protective coatings.

Acknowledgements

The authors wish to thank the Faculty of Chemical Technology, Hanoi University of Industry (HaUI), Vietnam for supporting this work.

Declaration of generative AI in scientific writing

Declaration of Generative AI in Scientific Writing

This manuscript utilized generative AI tools, namely ChatGPT (OpenAI) and Grammarly, to enhance language clarity, grammar, and overall readability.

• All AI-assisted edits were made under strict human oversight and control.

• These tools were not used to:

• Generate scientific content

• Interpret or analyze data

• Develop research questions

• Draw or formulate conclusions

The authors affirm that they are fully responsible for the intellectual content, scientific accuracy, and integrity of this manuscript.

CRediT Author Statement

Tuan Anh Nguyen: Conceptualization, Methodology, Investigation, Writing – Original Draft, Supervision, Project administration.

Van Hoan Nguyen: Formal analysis, Validation, Data curation, Visualization, Writing – Review & Editing.

References

[1] SC Pinto, G Gonçalves, S Sandoval, AM López-Periago, A Borras, C Domingo, G Tobias, I Duarte, R Vicente and PAAP Marques. Bacterial cellulose/graphene oxide aerogels with enhanced dimensional and thermal stability. *Carbohydrate Polymers* 2019; **230**, 115598.

[2] MA Masanabo, JT Keränen, SS Ray and NA Emmambux. Effect of cowpea lignocellulosic fibers as a low-value reinforcing filler on the properties of poly(butylene succinate-co-adipate) bio-composite foams. *Macromolecular Materials and Engineering*. 2025; **310(7)**, 2400369.

[3] N Sridhar, MSA Vallavi and T Mugilan. Synthesis and characterization of polyvinyl alcohol/Senna alata extract incorporated film for biomedical application. *Polymer Bulletin* 2024; **81(15)**, 13839-13862.

[4] F Liu, Y Zhang, X Xiao, Y Cao, W Jiao, H Bai, L Yu and Q Duan. Effects of polyvinyl alcohol content and hydrolysis degree on the structure and properties of extruded starch-based foams. *Chemical Engineering Journal* 2023; **472(7)**, 144959.

[5] W Guo, Y Hu, X Wang, P Zhang, L Song and W Xing. Exceptional flame-retardant cellulosic foams modified with phosphorus-hybridized graphene nanosheets. *Cellulose* 2019; **26(2)**, 1247-1260.

[6] WJ Lee, AJ Clancy, JC Fernández-Toribio, DB Anthony, ER White, E Solano, HS Leese, JJ Vilatela and MS Shaffer. Interfacially-grafted single-walled carbon nanotube/poly(vinyl alcohol) composite fibers. *Carbon* 2019; **146**, 162-171.

[7] A Rafique, KM Zia, M Zuber, S Tabasum and S Rehman. Chitosan functionalized poly(vinyl alcohol) for prospects biomedical and industrial applications: A review. *International Journal of Biological Macromolecules* 2016; **87(4)**, 141-154.

[8] D Zhang, D Meng, Z Ma, Z Zhang, H Ning and Y Wang. Synthesis of a novel organic-inorganic hybrid flame retardant based on $Ca(H_2PO_4)_2$ and hexachlorocyclotriphosphazene and its performance in polyvinyl alcohol. *Journal of Applied Polymer Science* 2020; **138(13)**, 50099.

[9] M Aslam, MA Kalyar and ZA Raza. Polyvinyl alcohol: A review of research status and use of polyvinyl alcohol based nanocomposites. *Polymer Engineering & Science* 2018; **58(2)**, 2119-2132.

[10] H Li, CW Wu, S Wang and W Zhang. Mechanically strong poly(vinyl alcohol) hydrogel with macropores and high porosity. *Materials Letters* 2020; **266**, 127504.

[11] SP Lin, KY Lo, TN Tseng, JM Liu, TY Shih and KC Cheng. Evaluation of PVA/dextran/chitosan hydrogel for wound dressing. *Cell Polymers* 2019; **38(11)**, 15-30.

[12] L Fan, H Yang, J Yang, M Peng and J Hu. Preparation and characterization of chitosan/gelatin/PVA hydrogel for wound dressings. *Carbohydrate Polymers* 2016; **146**, 427-434.

[13] K Kalantari, E Mostafavi, B Saleh, P Soltantabar and TJ Webster. Chitosan/PVA hydrogels incorporated with green synthesized cerium oxide nanoparticles for wound healing applications. *European Polymer Journal* 2020; **134(3)**, 109853.

[14] TA Nguyen, TH Nguyen, TTP Nguyen, MH Nguyen, MV Nguyen, NT Nguyen, DTY Oanh, TTT Bui, TV Ngo and XT Dam. Exploring graphene oxide and bacterial cellulose for Cr(VI) removal from water. *Vietnam Journal of Chemistry* 2025. https://doi.org/10.1002/vjch.70006

[15] TA Nguyen, DTY Oanh, MH Nguyen, TH Nguyen, TTP Nguyen, THN Le, MV Nguyen, TMH Pham, QT Nguyen. Research to develop the ability to remove As(III) ions in water of an environmentally friendly hybrid material based on bacterial cellulose and graphene oxide. *Vietnam Journal of Chemistry*. 2024; **62(5)**, 1-15.

[16] Y Wu, M Wang, Z Wang and J Wang. Green fabrication of robust and transparent PVA/BC/GO nanocomposite films with enhanced mechanical, thermal, and UV-shielding properties. *Carbohydrate Polymers* 2023; **317**, 120899.

[17] T Zhang, J Song and F Liu. Graphene oxide-bacterial cellulose hybrid aerogels for effective antibacterial and wound healing applications. *Materials Science and Engineering: C* 2021; **123**, 112020.

[18] A Kumar, RP Singh and S Pal. Fabrication of poly(vinyl alcohol)/bacterial cellulose/graphene oxide hybrid hydrogel for wound dressing. *International Journal of Biological Macromolecules* 2021; **183**, 1512-1520.

[19] L He, H Wang and H Liu. Multifunctional PVA/BC/GO membranes for food packaging with improved oxygen barrier and flame-retardant properties. *Food Packaging and Shelf Life* 2022; **33**, 100904.

[20] R Morales-Narváez and L Merkoçi. Nanomaterials for biosensing, imaging, and drug delivery. *Advanced Drug Delivery Reviews* 2020; **168**, 1-21.

[21] X Chen, S Zhang and Y Zhang. Preparation and characterization of PVA/BC/GO composite films

for biomedical applications. *Journal of Applied Polymer Science* 2022; **139(11)**, 51854.

[22] M Almasian and S Shahrokhian. Biocompatible nanocomposite films based on bacterial cellulose/graphene oxide/PVA for medical device coatings. *Materials Today Communications* 2021; **28**, 102635.

[23] J Wei, L Li and Q Wang. Flame retardancy and mechanical reinforcement in PVA-based nanocomposites via synergistic effects of bacterial cellulose and graphene oxide. *Polymer Degradation and Stability* 2021; **183**, 109490.

[24] Z Lin, Y Zhu and X Liu. Environmentally friendly polymer films reinforced with bacterial cellulose and graphene oxide for protective packaging. *ACS Sustainable Chemistry & Engineering* 2021; **9(1)**, 289-298.

[25] M Taghizadeh and B Saber-Samandari. PVA-based hydrogel incorporating BC and GO: Mechanical enhancement and sustained drug release. *European Polymer Journal* 2021; **142**, 110143.

[26] P Ma, Y Liu, S Wen, B He, X Ma, Q Huang, X Sun, W Gao and Y Bai. A bacterial cellulose nanocrystals-graphene oxide/ poly(vinyl alcohol) @vanillin composite fibers with efficient antibacterial activity and high strength for surgical suturing. *Advanced Healthcare Materials* 2025. https://doi.org/10.1002/adhm.202404511

[27] Y Wu, Q Zhang, F Li and L Chen. Green fabrication of robust and transparent PVA/BC/GO nanocomposite films with enhanced mechanical, thermal, and UV-shielding properties. *Carbohydrate Polymers* 2024; **317**, 120899.

[28] Q Yang, J Tan, S Tao, H Qiu, W Zhou, J Zhu, H Zhang, L Pei, T Zhou and J Wang. Fabrication and properties of conductive films based on bacterial cellulose and poly-N-isopropylacryla-mide-modified graphene oxide. *International Journal of Biological Macromolecules* 2024; **278(P2)**, 134867.

[29] IS Mir, A Riaz, J Fréchette, JS Roy, J Mcelhinney, S Pu, HK Balakrishnan, J Greener, LF Dumée and Y Messaddeq. Bacterial cellulose-graphene oxide composite membranes with enhanced fouling resistance for bio-effluents management. *npj Clean Water* 2024; **7(1)**, 111.

[30] L Feng, Y Shi, J Liu and T Huang. Recent progress on nanocellulose-based nanocomposites for environmental and energy applications. *Progress in Materials Science*. 2025; **140**, 101121